In situ observation of the periodical domain structure formation in KTiOPO$_4$

K. S. Buritskii, E. M. Dianov, V. A. Maslov, V. A. Chernykh, and E. A. Shcherbakov[a)]
Fiber Optics Research Center, General Physics Institute, Russian Academy of Sciences, 38 Vavilov Street, 117942 Moscow, Russia, CIS

The strain-induced periodical domain inversion in KTiOPO$_4$ (KTP) has been demonstrated *in situ* by means of the nonlinear light diffraction. The temperature of 730 °C was found to be the starting point of the opposite sign domains growth under the heating of $-Z$ KTP substrate (rate 70 °C/s) with the periodical SiO$_2$ mask. The depth of the fabricated domain-reversed structure of the 5.5 μm period was measured to be 4.5 μm. © *1996 American Institute of Physics.*
[S0021-8979(95)01922-7]

Compact blue and green coherent light sources are required for many applications such as optical data storage, laser printing, medicine, and other. One of the ways to realize these light sources is the using of the second-harmonic generation (SHG) of GaAlAs laser diodes. In particular, the quasiphase-matched (QPM) SHG in optical waveguides produced in the such nonlinear crystals as LiNbO$_3$, LiTaO$_3$, and KTiOPO$_4$ (KTP) is an attractive solution of effective light frequency conversion.[1–3]

QPM is based on periodical modulation of the second-order nonlinear polarization along the optical waveguide. The period Λ of the modulation for a fixed pump wavelength λ_ω is determined by the pump n_ω^* and SH $n_{2\omega}^*$ effective refractive indexes and is equal to

$$\Lambda = \lambda_\omega / 2(n_{2\omega}^* - n_\omega^*).$$

The efficiency of the QPM SHG is mainly determined by the modulation index of the nonlinear susceptibility, and the periodically modulated ferroelectric polarization (reversed-domain structure) allows to reach the most effective nonlinear interaction.

Recently, the generation of as much as 400% W^{-1} cm^{-2} normalized efficiency of blue light has been demonstrated in QPM KTP waveguides.[4,5] The key parameter of the nonlinear conversion efficiency is the spatial overlap of the waveguide modes for pump and SH waves and the periodical domain depth distribution.[6] It requires the use of special methods of precise domain control in the fabricated optical waveguides.

Some techniques including the selective chemical etching, electrostatic toning,[7] and optical observations by using nonlinear Talbot effect[8] are currently applied to characterize the periodical domain structures in the different crystals. The last-named method makes it possible to study *in situ* the process of the domain inversion.

In this communication we report, for the first time, on the application of the nonlinear Talbot diffraction to the investigation *in situ* of the periodically inverted ferroelectric domains formation in a KTP crystal.

The techniques used for domain inversion in LiNbO$_3$, LiTaO$_3$, and KTP can be separated into two principal groups. The first one is based on diffusion[1] or ion exchange;[3] some elements and the refractive index of the crystals are simultaneously changed in these cases. The second group includes the strain[9,10] and electric-field-induced methods,[11] and also electron-beam writing[12] when the refractive index of the crystal is practically not changed during the process. The domain grating fabricated by the second group of the methods can be easily revealed by nonlinear light diffraction.

In this case, the modulated wave of nonlinear polarization, arising in a nonlinear crystal with periodically inverted domains, and hence with modulated nonlinear coefficient, leads to the modulation of the SH wave complex amplitude. The intensity of the SH wave generated in the crystal regions of lengths L_1, L_2 having equal/opposite signs of the nonlinear coefficient can be easily calculated.[13] The corresponding SH diffraction pattern can be observed in the far or near field. The examination of the appropriate intensity distribution makes it possible to characterize the domain structure.

We have studied the far- and near-field SH distributions for the pump beam directed from the bulk to the domain-inverted layer, and the incidence plane for the pump wave being parallel to the domain walls (see Fig. 1). The input angle and beam position are chosen in such a manner that the propagation in the bulk and in the inverted-domain area occurs without reflection [Fig. 1(b)].

The calculated depth dependence of the SH at the output end face for a uniform plane pump wave[13] is given by the equation

$$I_{2\omega} \propto \frac{3}{2} + \frac{1}{2} \cos\left(\frac{\Delta k L}{\cos \alpha}\right) - 2 \cos\left(\frac{\Delta k L}{2 \cos \alpha}\right) \cos\left[\frac{\Delta k}{2}\left(\frac{L}{\cos \alpha} - \frac{2d - 2z}{\sin \alpha}\right)\right] \quad (1)$$

for propagation through the bulk and inverted segment, and

$$I_{2\omega} \propto \sin^2\left(\frac{\Delta k L}{2 \cos \alpha}\right) \quad (2)$$

for the bulk and noninverted region, where L is crystal length, $\Delta k = 2k_\omega - k_{2\omega}$, $k = 2\pi/\lambda$, and d is the inverted do-

a)Electronic mail: shcher@fo.gpi.ac.ru

(a)

Inverted domains

KTP

SiO$_2$ mask
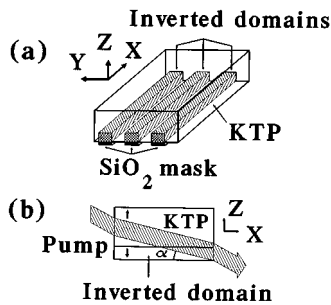
(b) KTP

Pump

Inverted domain

FIG. 1. Schematic of inverted domain grating illumination for the domain revealing: (a) SiO$_2$ grating; (b) beam position for near-field observation.

main depth. Thus, the maximum and minimum intensities in the distribution observed for $d > L_c \sin \alpha$, where $L_c = \pi/\Delta k$, are proportional to

$$\left[1 \pm \cos \left(\frac{2\Delta k L}{2 \cos \alpha} \right) \right]^2, \qquad (3)$$

but for the noninverted region SH intensity is depth independent [Eq. (2)]. Choosing the angle α so that $\Delta k L/\cos \alpha \neq \pi n$ ($n = 0,1,...$), the space modulation of the SH intensity in the depth direction can be observed. Moreover, the maximum SH intensity in place of the inverted domain has to exceed of this one in the noninverted region. So, the output intensity of the SH wave will be modulated while the pump wave will remain a plane wave.

The experiments were carried out on the flux-grown KTP substrates with the conductivity of $5 \times 10^{-7} \ \Omega^{-1} \text{cm}^{-1}$. The polished plates were $2 \times 6 \times 1 \ \text{mm}^3$ in size along X, Y, Z crystallographic axes, respectively. The input and output crystal end faces (XZ planes) were also polished. The periodical SiO$_2$ mask of 100 Å thickness with a period $L = 5.5 \ \mu$m (1.7 μm SiO$_2$ stripe width) was fabricated by photo-lithography on the $-Z$ crystal surface.

The scheme of the experimental setup is shown in Fig. 2. A Q-switched mode-locked Nd:YAG laser was used as a pump source. Average pump power ($\lambda = 1.064 \ \mu$m) was equal to 1 W, pulse duration to 800 ps, and duration of the pulse train to 400 ns at repetition rate of 6.3 kHz. Radiation
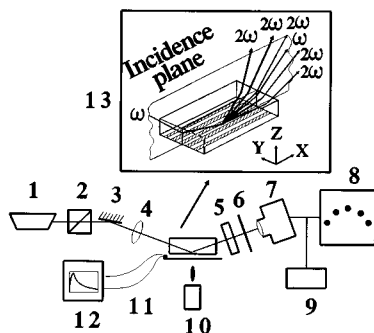
FIG. 2. Experimental arrangement of periodically inverted domain revealing during the fabrication process: (1) Nd:YAG laser; (2) polarizer; (3) mirror; (4) lens; (5) IR-cut filter; (6) screen; (7) TV camera; (8) monitor; (9) VCR; (10) H$_2$–O$_2$ burner; (11) thermocoupler; (12) XY plotter; (13) KTP crystal with SiO$_2$ mask at Pt plate.
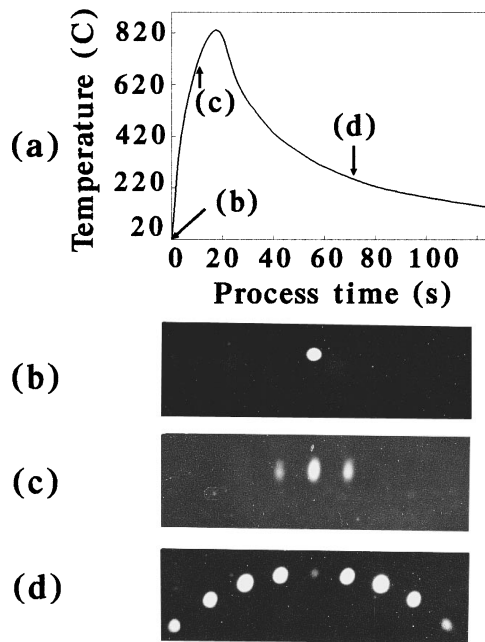
FIG. 3. Far-field SH diffraction patterns at different stages of the strain-induced domain grating fabrication: (a) KTP substrate temperature vs time; (b) SH image before substrate heating; (c) domain inversion start temperature $T = 730$ °C; (d) $T = 250$ °C at substrate cooling stage.

was polarized along Z crystal axes. The pump beam was focused into the substrate through the input end face by a 15 cm focus lens, the incidence angle α being equal 20° to ensure total internal reflection for the waves with the frequencies ω and 2ω. Far-field SH distribution was observed through the screen 5 cm away from the output end face. The pattern on the screen was imaged with a TV camera and recorded by a VCR.
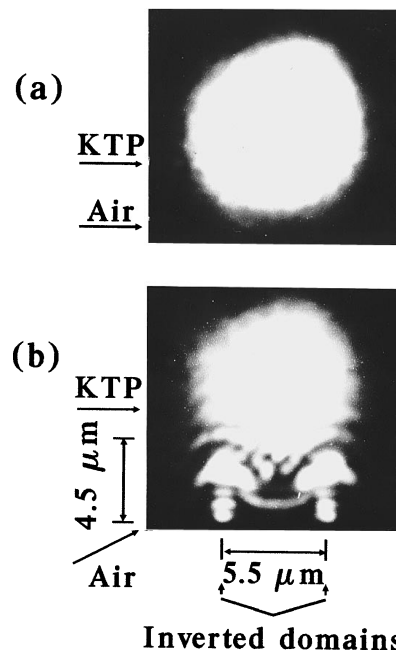
FIG. 4. Near-field SH images for the inverted domain structure: (a) before inversion; (b) fabricated grating.

The KTP substrate was placed on the polished Pt plate 0.3 mm thick, which was heated by H_2–O_2 burner up to 840 °C [Fig. 3(a)] to induce a strain in KTP because of the different thermal-expansion coefficients of the periodical SiO_2 mask and crystal.

The far-field SH ($e+e\rightarrow e$ interaction) distributions at different stages of the process are presented in Figs. 3(b)–3(d). We did not observe the pump wave diffraction. This testifies that there was no visible refractive index change in the structure fabricated. As can be seen [Fig. 3(c)] the inversion process starts at the substrate temperature $T=730$ °C. The far-field pattern during the substrate cooling [Fig. 3(d)] indicates the formation of the domains grating.

Appropriate near-field SH images are shown in Fig. 4. In this case, the pump beam was focused into the substrate near the output end face with a $5\times$ microobjective. The near-field distributions were analyzed with a $40\times$ microobjective (NA $=0.65$). It can be seen that a periodical domain-inverted structure 4.5 μm in depth with 5.5 μm period was formed as a result of the substrate treatment described above.

It is necessary to point out that the mechanism of the periodical domain structure formation in KTP is not now clear, but the parameters of the fabricated structures are strongly dependent on the substrate conductivity and on the heating rate. In particular, the deep periodical domain structures were produced under a heating rate of more than 65 °C/s.

In conclusion, we have demonstrated *in situ* the periodical domain inversion by the strain-induced method in KTP. It was shown that an examination of the nonphase-matched SHG enables one to control the parameters of periodically inverted domain structures during the fabrication.

[1] S. Miyazawa, J. Appl. Phys. **50**, 4599 (1979).
[2] K. Yamamoto, K. Mizuuchi, and T. Taniuchi, Appl. Phys. Lett. **58**, 2732 (1991).
[3] C. J. van der Poel, J. D. Bierlein, J. B. Brown, and S. Colak, Appl. Phys. Lett. **57**, 2074 (1990).
[4] J. D. Bierlein, in *Digest of Compact Blue-Green Lasers Topical Meeting* (Optical Society of America, Washington, DC, 1992), paper FC2.
[5] D. Eger, M. Oron, M. Katz, and A. Zussman, Appl. Phys. Lett. **64**, 3208 (1994).
[6] M. J. Jongerius, R. R. Drenten, and R. B. G. Droste, Philips J. Res. **46**, 231 (1992).
[7] F. Laurell, M. G. Roelofs, W. Bindloss, H. Hsiung, A. Suna, and J. D. Bierlein, J. Appl. Phys. **71**, 4664 (1992).
[8] K. S. Buritskii, V. A. Chernykh, E. M. Dianov, V. A. Maslov, and E. A. Shcherbakov, in *Digest of Compact Blue-Green Lasers Topical Meeting* (Optical Society of America, Washington, DC, 1994), paper CThB7.
[9] M. Fujimura, T. Suhara, and N. Nishihara, Electron. Lett. **27**, 1207 (1991).
[10] K. S. Buritskii, V. A. Chernykh, E. M. Dianov, V. A. Maslov, and E. A. Shcherbakov, Sov. Lightwave Commun. **3**, 111 (1993).
[11] M. Yamada, N. Nada, M. Saitoh, and W. Watanabe, Appl. Phys. Lett. **62**, 435 (1993).
[12] H. Ito, C. Takyu, and H. Inaba, Electron. Lett. **27**, 1221 (1991).
[13] F. R. Nash, E. H. Turner, P. M. Brindenbaugh, and J. M. Dziedzic, J. Appl. Phys. **43**, 1 (1972).

Published without author corrections